Nanoscale

Accepted Manuscript

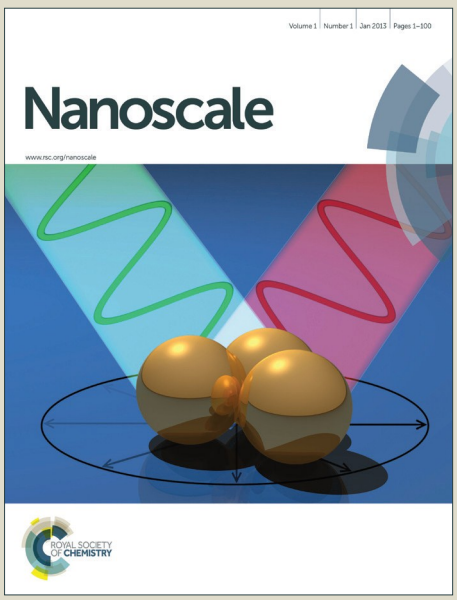

ROYAL SOCIETY OF CHEMISTRY

www.rsc.org/nanoscale

Nanoscale

COMMUNICATION

High performance three-phase enzyme electrode based on superhydrophobic mesoporous silicon nanowire arrays for glucose detection

Received 00th January 20xx,
Accepted 00th January 20xx

DOI: 10.1039/x0xx00000x

www.rsc.org/

Chenlong Xu[a#], Zhiqian Song[b#], Qun Xiang[a], Jian Jin[c] and Xinjian Feng[bc]*

We describe here a high performance oxygen-rich three-phase enzyme electrode based on superhydrophobic mesoporous silicon nanowire arrays for glucose detection. We demonstrate that its linear detection upper limit is 30 mM, more than 15 times higher than that can be obtained on the normal enzyme-electrode. Notably, the three-phase enzyme electrode output is insensitive to the significant oxygen level fluctuation in analyte solution.

Introduction

Many insects can remain submerged in water for a long time in nature. The micro-/nanoscale hair arrays on parts of their body play a key role in the underwater respiration, because the array structures form nature superhydrophobic surfaces that can carry air layer while submerged in water and serve the insects as a physical gill.[1,2] Inspired from the top morphologies of non-wetting natural surfaces, a wide variety of artificial substrates with superhydrophobicity have been created.[3-13] They are opening applications in many areas, such as rapid gas transport under water,[14] carbon dioxide or marine methane capture,[15,16] low friction fluid transport and drag reduction on ship hulls.[2,17,18] Besides, the air-retaining capability of superhydrophobic surface structure inspires innovative resolutions in areas where the oxygen-deficit is the key problem.

The development of accurate oxidase-based biosensors is important for the diagnosis and control of worldwide diabetes and other health problems.[19-28] First-generation biosensors, which rely on the use of natural oxygen cosubstrate and the measurement of peroxide production in oxidase catalytic bioreactions, have the advantage of being simpler, especially when miniaturized devices are concerned.[21,29,30] However, their broad application has been largely limited by the relatively low (< 0.2 mM) and significantly fluctuant oxygen levels in analyte solutions, which compromise the detection linearity, sensitivity and accuracy. To achieve wide linear detection range and accuracy, analyte solution dilution or mass-transport-limiting membrane has been employed to ensure the oxygen/analyte ratio at the enzymatic reaction interface.[29,30] However, such detection suffers from low sensitivity due to the restricted H_2O_2 formation (low analyte concentration at the assay interface). Another approach reported to address the oxygen-deficit problem is using oxygen-rich binders, such as poly (chlorotrifluorethylene) oil as an internal source of oxygen.[31,32] Oxygen needed at the enzymatic active sites is still supplied via liquid phase with the slow diffusion coefficients, and the oxidase kinetic is oxygen level restricted.

In this paper, inspired from the air-retaining capability of surface array structures of submerged insects, we addressed the oxygen-deficit problem by developing a novel three-phase enzyme (TPE) electrode system based on superhydrophobic aligned mesoporous silicon nanowire arrays (mpSiNWAs) substrate. Sufficient and constant oxygen at the enzymatic reaction interface was supplied from air phase with the high diffusion coefficients. Based on this TPE-electrode, we presented a linear detection range up to 30 mM with good sensitivity. Furthermore, the electrode output is insensitive to the significant oxygen level fluctuation in solution.

Experimental Section

Chemical

Silicon (100) wafers (p-type, boron-doped, 1-5 mΩ•cm, 500-550 μm thick) were purchased from Ultrasil Corp. Hydrofluoric acid (HF, ⩾40%), silver nitrate ($AgNO_3$, ⩾99.8%), H_2O_2 (⩾ 30%), sulfuric acid (H_2SO_4), nitric acid (HNO_3, 65% to 68%), potassium chloride (KCl, ⩾99.8%), acetone, ethanol, toluene, acetic acid, chitosan, glucose and glutaraldehyde (25%) were purchased from Sinopharm Chemical Reagent Co., Ltd.

[a] NEST Lab, Department of Chemistry, College of Science, Shanghai University, Shanghai, 200444, P. R. China
[b] College of Chemistry, Chemical Engineering and Materials Science, Soochow University, Suzhou 215123, P. R. China. E-mail: xjfeng@suda.edu.cn
[c] Suzhou Institute of Nano-Tech and Nano-Bionics, Chinese Academy of Sciences, Suzhou, 215123, P. R. China
Electronic Supplementary Information (ESI) available. See DOI: 10.1039/x0xx00000x
[#] These authors contributed equally to this work.

(Shanghai, China). Glucose oxidase (GOx), and trichloro(octadecyl)silane (OTS) were purchased from Sigma (USA). All chemicals were directly used without further purification. All solutions were prepared with Milli-Q water except especially mentioned.

Preparation of mpSiNWs and fabrication of TPE-electrode

Silicon wafers were cut into 2.4 cm × 1.2 cm pieces and sonicated in ethanol, acetone, and water for 15 min, respectively. Then the cleaned Si wafer was immersed in H_2SO_4 and H_2O_2 (v/v 3:1) solution for 10 min to remove organic materials. After each cleaning step, the wafer pieces were rinsed with excess water. The cleaned Si wafer pieces were then immersed in 8% HF solution for 10 min to form H-terminated surface. The H-terminated wafer was immediately put into the solution containing 8% HF and 8.3 mM $AgNO_3$ to coat a uniform layer of Ag nanoparticles. Successively, the wafer was immersed in the etchant solution composed of 8% HF and 0.27 M H_2O_2 for 30 min under room temperature. Upon removal from the etch bath, the wafer was dipped in HNO_3 to dissolve the deposited Ag film. Lastly, the resulting arrays were thoroughly washed with water and dried in a vacuum. The mpSiNWAs substrates with lengths of 2.8 and 4.5 µm (shown in Fig. S2A and B) were obtained by using etching time of 5 and 12 min respectively.

A Pt film was deposited on the as-prepared mpSiNWs by sputter technique. Then the superhydrophobicity of the mpSiNWs was received by immersing the sample in toluene solution of 2 mM OTS for 1 hour. In parallel, a solution of GOx (1 wt. % in PBS solution), chitosan (1 wt.% in acetic acid) and glutaraldehyde (0.58 wt.% in DI water) with the volume ratio of 1:1:13 was mixed thoroughly. 0.15 mL of the resulting mixture was drop cast onto the surface of the Pt deposited superhydrophobic mpSiNWs substrate with size of 0.5 cm^2. After dried naturally, the sample was used as working electrode. In electrochemical experiments, the as-prepared TPE-electrode was dipped upright in the electrolyte solution with the GOx/chitosan area submerged and a portion of the superhydrophobic area kept above the liquid level simultaneously.

Preparation of normal two-phase enzyme electrode

A glass carbon (GC) electrode of 3 mm in diameter was mechanically polished with 1, 0.3 and 0.05 mm alumina slurry and then sequentially sonicated in water, ethanol and water for several minutes. Cleaned GC electrodes were dried with nitrogen stream. In parallel, a solution of GOx (1 wt. % in PBS solution), chitosan (1 wt.% in acetic acid) and glutaraldehyde (25 wt.% in DI water) with the volume ratio of 10:10:3 was mixed thoroughly. The normal two phase electrode was obtained by casting the mixed solution of 3 µL onto the GC electrode, which was then covered to allow slow evaporation and the film formation at the electrode surface.

Instrumentation

The microstructures of mpSiNWs were investigated by using a field-emission scanning electron microscope (FESEM, HITACHI-S4800, Japan). Morphologies of GOx based electrode were investigated by using environmental scanning electron microscope (ESEM, FEI Quanta 400 FEG, USA). The transmission electron microscopy (TEM) image were taken using Tecnai F20 (FEI, Hillsboro, OR, USA) microscope at an accelerating voltage of 200 kV. Energy Dispersive X-ray (EDX) analysis was performed using environmental scanning electron microscope (ESEM, FEI Quanta 400 FEG, USA).

The sputter-depositing of Pt was carried out by EMITECH-K550X apparatus. The sputtering conditions were as follows: the sputtering current was 25 mA, the sputtering pressure was 5 Pa, and the sputtering time was 3 min. All electrochemical experiments were carried out with CHI 660E (CHI Instruments Inc., Austin, USA). A conventional three-electrode system was used in this work. MpSiNWAs based TPE-electrodes were used as the working electrodes, and a platinum wire and an Ag/AgCl (3 M KCl) electrode were used as the counter and the reference electrodes, respectively. Phosphate buffer of 0.2 M (pH 7.2) was employed as the supporting electrolyte. The assays using normal two phase electrode and the data analysis were carried out in the same way as the TPE-electrode.

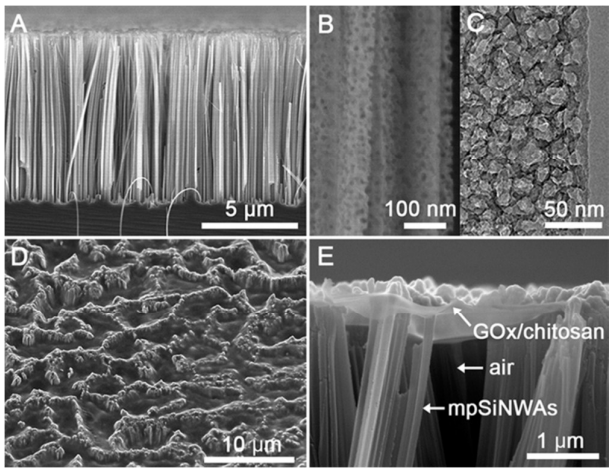

Fig. 1 (A) and (B) are FE-SEM side views of the mpSiNWAs substrate prepared with 30 min etching at low and high magnifications, respectively. (C) TEM image of the mesoporous silicon nanowires. (D) E-SEM top view of the TPE-electrode with a 45° titling angle. (E) E-SEM side view of the TPE-electrode.

Results and discussion

The mpSiNWAs substrate was prepared via a metal-assisted chemical etching approach.[33,34] Fig. 1A and B show the field-emission scanning electron microscope (FESEM) images of the mpSiNWAs substrate prepared after 30 min chemical etching. The nanowires are uniform and vertically oriented with a length of about 8.5 µm. Pores with a diameter of appropriately

Nanoscale

COMMUNICATION

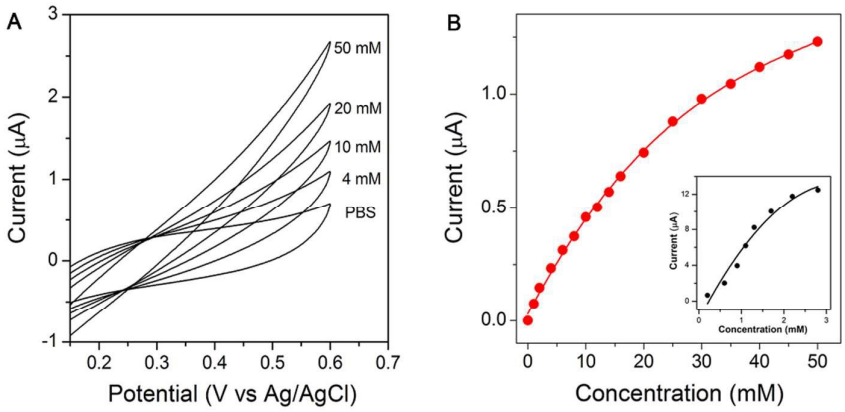

Fig. 2 (A) Current-potential curves of the TPE-electrode for in the presence of glucose with various concentrations. (B) Plots of anodic current derived from (A) at +0.5 V (vs. Ag/AgCl) versus the glucose concentration for the TPE-electrode. Inset in (B) shows the plot of anodic current at +0.5 V (vs. Ag/AgCl) versus the glucose concentration for normal enzyme electrode. Scan rate: 50 mV/s.

15 nm were observed to distribute homogeneously along the nanowires. Transmission electron microscopy (TEM) micrograph shown in Fig. 1C illustrates the pore structure fills the inside of whole nanowire. The well separation of Si nanowire and the pores inside offer the substrate an opportunity to retain the large amount of oxygen for enzymatic reaction. On the top of mpSiNWAs, electrocatalyst Pt was immobilized via sputter deposition and its presence was confirmed by Energy Dispersive X-ray analysis (Fig. S1A and B). The Pt-decorated nanowire substrate was further treated with OTS. Fig. S2 shows spherical water droplet placed on the surface, indicating a superhydrophobic nature of the substrate was achieved. Based on this substrate,

TPE-electrode was constructed by depositing a thin layer (~400 nm thick) of GOx/chitosan composite onto the surface. Fig. 1D and E are environmental scanning electron microscope (ESEM) top and side views of the as-prepared TPE-electrode surface, respectively. Only the top part of silicon nanowires is covered by the GOx/chitosan composite layer. Such electrode structure facilitates the free diffusion of oxygen and glucose, respectively from the air and liquid phases to the oxidase active sites. Here, H_2O_2 that is proportional to the glucose concentration is generated and anodized on the Pt surface to give the fast electrode response.

The as-prepared TPE-electrode is used for glucose detection. Cyclic voltammograms (CVs) (Fig. 2A) shows the anodic current increasing with the glucose concentration. Fig. 2B shows the calibrated curve of current as a function of glucose concentration. A linear detection range up to 30 mM with a correlation coefficient (R) of 0.993 is achieved. As illustrated in the insert of Fig. 2B, control experiment based on the normal enzyme electrode (glass carbon electrode) that has the solid-liquid two-phase assay interface shows a linear detection range only up to about 2 mM. The remarkable improvement of linear detection range achieved in TPE-electrode can be attributed to the air retaining capability of the mpSiNWAs electrode substrate. When the TPE-electrode is in contact with analyte solution, the top GOx layer will be wetted. However, water cannot enter the porous nanowire array electrode substrate due to its super-hydrophobicity. This leads to the formation of the solid-liquid-air three-phase assay interface. Glucose diffuses from bulk solution to the assay interface and is oxidized by GOx. The reduced GOx can be regenerated efficiently, because sufficient oxygen is available at the interface, i.e. the oxidase kinetic is no longer oxygen level limited. As a result, H_2O_2 that is proportional to the glucose concentration can be produced and electro-oxidized on the Pt surface to give the electric signal. Thus, the mpSiNWAs based TPE-electrode solved the oxygen deficit problem, and a wide linear detection range is obtained.

The air retaining layer plays an important role in the performance enhancement in TPE-electrode. The influence of mpSiNWAs length on the electrode response was further investigated. As shown in Fig. S3, the upper limit of the detection range of the as-prepared electrode increases linearly with the increase of mpSiNWAs length from 2.8 μm to 8.5 μm. These results confirmed the superhydrophobic mpSiNWAs electrode substrate plays an important role in the device performance. The increasing length of the mesoporous

nanowire arrays can enhance the oxygen retaining capability of electrode substrate, and enlarge the linear detection range. In order to separate the effect of the high surface area of the SiNW from increased oxygen availability, we made an enzyme electrode using the 8.5 μm SiNW array without the functionalization of OTS and then operated anodic detection of glucose. As shown in Fig. S4, the linear detection upper limit of the hydrophilic SiNW electrode is only about 2 mM, which is similar to that of the normal enzyme electrode made with a GC electrode. This result further confirmed that the significant increase in the linear range should be attributed to the much enhanced oxygen availability at the assay interface.

We further evaluated the effect of oxygen level fluctuation on the bioassay accuracy using the mpSiNWAs based TPE-electrode. The buffer solution was bubbled with argon for 30 min to remove oxygen before the measurement. Then, 2 mM glucose was added and the amperometric response of the TPE-electrode was recorded. The current increased immediately with the addition of glucose and then kept almost constant after that (Fig. 3 curve a), indicating the TPE-electrode response is not influenced by the oxygen level fluctuation in the assay solution. Control experiments were also carried out on the normal enzyme electrode. As shown in Fig. 3 curve b, the current exhibited a quick small increase caused by the residual oxygen in the solution, followed by a slow rise resulted from the continuously increasing oxygen content through diffusion from air under stirring condition. This result indicates the variation of oxygen level in the solution has a strong influence on the assay accuracy of the normal enzyme electrodes. These results confirm the oxygen involved in oxidase-catalytic bioreaction at the assay interface of TPE-electrode is supplied constantly and sufficiently from air phase. Thus, the detection accuracy is insensitive to the oxygen level variation in analyte solution.

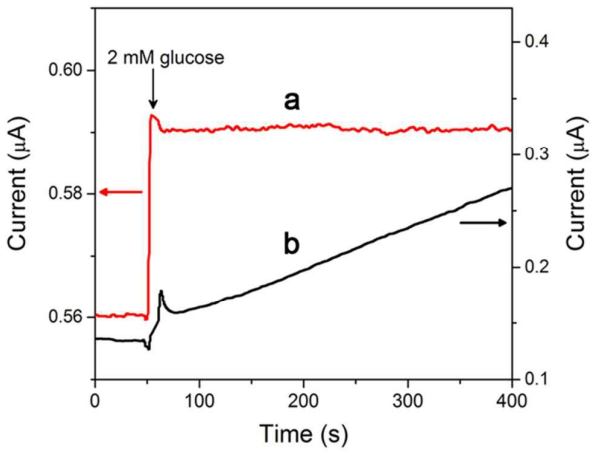

Fig. 3 Amperometric response of (a) TPE-electrode and (b) normal enzyme electrode to 2 mM glucose solution upon switching from the oxygen-deficit to oxygen-rich environment (Applied potential: +0.5 V). The current output remains constant with time for TPE-electrode, but keeps increasing for normal one. This confirmed that oxygen level variation has no influence on the detection accuracy of TPE-electrode.

Fig. S5 shows a typical amperometric response of the TPE-electrode with successive addition of glucose to the buffer solution under stirring. The current increased immediately with addition of glucose and reached a steady-state. The average response time of the TPE-electrode is less than 6 s (reaching 95% of steady-state current). This fast response could be attributed to the barrier-free enzyme electrode surface, which enables glucose molecules to diffuse freely from bulk solution to the assay interface. The detection limit is estimated to be about 25 μM (based on S/N = 3). The stability of the TPE-electrode was evaluated by 20 times continuous measurements in the presence of different glucose concentrations (Fig. 4). The relative standard deviation observed are 1.03%, 0.58% and 1.32%, respectively, for 5 mM, 10 mM, and 20 mM glucose, indicating a good stability and repeatability of the TPE-electrode.

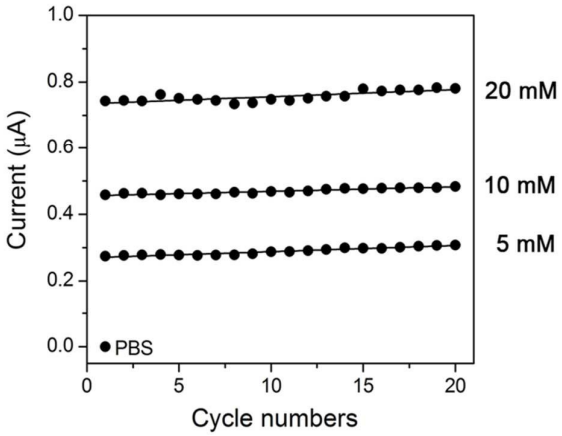

Fig. 4 Successive 20 times CV measurements of the TPE-electrode in the presence of 5 mM, 10 mM and 20 mM glucose. Current was obtained at 5 s following the potential step. Applied potential: +0.5 V.

Conclusions

In summary, we have developed a biomimetic oxygen-rich TPE-electrode that was fabricated via depositing a thin GOx/chitosan composite layer on electrocatalyst Pt decorated superhydrophobic mpSiNWAs electrode substrate. Such enzyme electrode has a solid-liquid-air three-phase assay interface in which oxygen can be supplied rapidly from air phase. Based on this electrode, a wider linear detection range with fast response, good sensitivity and accuracy was achieved. Such novel strategy provides a practical approach for the fabrication and broad applications of the simpler and reliable first-generation biosensor.

Acknowledgements

This work was supported by the National Natural Science Foundation of China (21371178) and the Chinese Thousand Youth Talents Program (YZBQF11001).

Notes and references

1 A. Balmert, H. Florian Bohn, P. Ditsche-Kuru and W. Barthlott, *J. Morphol.*, 2011, **272**, 442.
2 P. Ditsche-Kuru, E. S. Schneider, J. E. Melskotte, M. Brede, A. Leder and W. Barthlott, *Beilstein J. Nanotechnol.*, 2011, **2**, 137.
3 A. B. D. Cassie and S. Baxter, *Trans. Faraday Soc.*, 1944, **40**, 546.
4 X. Deng, L. Mammen, H.-J. Butt and D. Vollmer, *Science*, 2012, **335**, 67.
5 H. Y. Erbil, A. L. Demirel, Y. Avci and O. Mert, *Science*, 2003, **299**, 1377.
6 L. Feng, S. H. Li, Y. S. Li, H. J. Li, L. J. Zhang, J. Zhai, Y. L. Song, B. Q. Liu, L. Jiang and D. B. Zhu, *Adv. Mater.*, 2002, **14**, 1857.
7 X. J. Feng and L. Jiang, *Adv. Mater.*, 2006, **18**, 3063.
8 A. Lafuma and D. Quere, *Nat.Mater.*, 2003, **2**, 457.
9 K. Liu, X. Yao and L. Jiang, *Chem. Soc. Rev.*, 2010, **39**, 3240.
10 T. L. Liu and C.-J. C. J. Kim, *Science*, 2014, **346**, 1096.
11 Y. Lu, S. Sathasivam, J. Song, C. R. Crick, C. J. Carmalt and I. P. Parkin, *Science*, 2015, **347**, 1132.
12 S. Farsinezhad, P. R. Waghmare, B. D. Wiltshire, H. Sharma, S. Amiri, S. K. Mitra and K. Shankar, *Rsc Adv*, 2014, **4**, 33587.
13 Z. Li, J. Wang, Y. Zhang, J. Wang, L. Jiang and Y. Song, *Appl. Phys. Lett.*, 2010, **97**,233107.
14 J. Wang, Y. Zheng, F.-Q. Nie, J. Zhai and L. Jiang, *Langmuir*, 2009, **25**, 14129.
15 X. Chen, Y. Wu, B. Su, J. Wang, Y. Song and L. Jiang, *Adv. Mater.*, 2012, **24**, 5884.
16 M. Paven, P. Papadopoulos, S. Schottler, X. Deng, V. Mailander, D. Vollmer and H. J. Butt, *Nat. Commun.*, 2013, **4**, 2512.
17 M. N. Kavalenka, F. Vullers, S. Lischker, C. Zeiger, A. Hopf, M. Rohrig, B. E. Rapp, M. Worgull and H. Holscher, *ACS Appl. Mater. Interfaces*, 2015, **7**, 10651.
18 N. J. Shirtcliffe, G. McHale, M. I. Newton and Y. Zhang, *ACS Appl. Mater. Interfaces*, 2009, **1**, 1316.
19 L. C. Clark and C. Lyons, *Ann. N. Y. Acad . Sci.*, 1962, **102**, 29.
20 S. J. Updike and G. P. Hicks, *Nature*, 1967, **214**, 986.
21 G. G. Guilbaul and G. J. Lubrano, *Anal. Chim. Acta.*, 1973, **64**, 439.
22 A. E. G. Cass, G. Davis, G. D. Francis, H. A. O. Hill, W. J. Aston, I. J. Higgins, E. V. Plotkin, L. D. L. Scott and A. P. F. Turner, *Anal. Chem.*, 1984, **56**, 667.
23 A. Heller, *Acc. Chem. Res.*, 1990, **23**, 128.
24 Y. Xiao, F. Patolsky, E. Katz, J. F. Hainfeld and I. Willner, *Science*, 2003, **299**, 1877.
25 C. Shan, H. Yang, J. Song, D. Han, A. Ivaska and L. Niu, *Anal. Chem.*, 2009, **81**, 2378.
26 N. J. Ronkainen, H. B. Halsall and W. R. Heineman, *Chem. Soc. Rev.*, 2010, **39**, 1747.
27 H. He, X. Xu, H. Wu and Y. Jin, *Adv. Mater.*, 2012, **24**, 1736.
28 M. S. Thakur and K. V. Ragavan, *J. Food Sci. Technol.*, 2013, **50**, 625.
29 A. Heller and B. Feldman, *Chem. Rev.*, 2008, **108**, 2482.
30 J. Wang, *Chem. Rev.*, 2008, **108**, 814.
31 J. Wang and F. Lu, *J. Am. Chem. Soc.*, 1998, **120**, 1048.
32 J. Wang, J. W. Mo, S. F. Li and J. Porter, *Anal. Chim. Acta.*, 2001, **441**, 183.
33 H. Chen, R. Zou, H. Chen, N. Wang, Y. Sun, Q. Tian, J. Wu, Z. Chen and J. Hu, *J. Mater. Chem.*, 2011, **21**, 801.
34 Y. Qu, H. Zhou and X. Duan, *Nanoscale*, 2011, **3**, 4060.